Mon. Not. R. Astron. Soc. **000**, 000–000 (0000) Printed 5 February 2008 (MN LATEX style file v2.2)

Axisymmetric black hole accretion in the Kerr metric as an autonomous dynamical system

Sanghamitra Goswami,[1⋆] Saba Nashreen Khan,[2]† Arnab K. Ray[3]‡ and Tapas K. Das[4]§
[1] *Department of Physics, Indian Institute of Technology Bombay, Powai, Mumbai 400076, India*
[2] *Department of Physics, Indian Institute of Technology Delhi, Hauz Khas, New Delhi 110016, India*
[3] *Inter–University Centre for Astronomy and Astrophysics, Post Bag 4, Ganeshkhind, Pune University Campus, Pune 411007, India*
[4] *Harish–Chandra Research Institute, Chhatnag Road, Jhunsi, Allahabad 211019, India*

5 February 2008

ABSTRACT
In a stationary, general relativistic, axisymmetric, inviscid and rotational accretion flow, described within the Kerr geometric framework, transonicity has been examined by setting up the governing equations of the flow as a first-order autonomous dynamical system. The consequent linearised analysis of the critical points of the flow leads to a comprehensive mathematical prescription for classifying these points, showing that the only possibilities are saddle points and centre-type points for all ranges of values of the fixed flow parameters. The spin parameter of the black hole influences the multitransonic character of the flow, as well as some of its specific critical properties. The special case of a flow in the space-time of a non-rotating black hole, characterised by the Schwarzschild metric, has also been studied for comparison and the conclusions are compatible with what has been seen for the Kerr geometric case.

Key words: accretion, accretion discs – black hole physics – hydrodynamics

1 INTRODUCTION

From a mathematical perspective, problems in astrophysical accretion fall under the general class of nonlinear dynamics. This occasions no surprise, because accretion, after all, describes the dynamics of a compressible astrophysical fluid, and the fundamental governing equations of such a problem are nonlinear in nature (Landau & Lifshitz 1987). One of the general issues that is addressed in accretion studies is the physics of the accretor itself, whose gravitational attraction sustains the global inflow process. This is especially important if the accretor is a black hole, which by its very definition is never amenable to any direct physical observation, and, therefore, its properties can only be known by the gravitational influence it exerts on the neighbouring structure of space-time.

If the accretor is a black hole, the infalling matter has to reach the event horizon on a relativistic scale of velocity, and arguments in favour of this contention have, by now, gained widespread currency (Begelman 1978; Brinkmann 1980; Shapiro & Teukolsky 1983; Chakrabarti 1990). Given physically sensible boundary conditions, this can only imply that at one stage the flow of matter will become transonic, i.e. its flow speed will grow from subsonic values to supersonic values, and in doing so, it will at some point match the speed of acoustic propagation in the fluid. This transition can happen continuously, as in smooth transonic solutions (Chakrabarti 1990), or discontinuously, as in shocks (Chakrabarti 1989, 1990). In accretion studies both possibilities have been subjected to concerted investigation.

Frequently it happens that the transonic feature is exhibited more than once in the phase portrait of stationary solutions, i.e. the flow will be multitransonic. This is particularly true in axisymmetric rotational flows (Abramowicz & Zurek 1981; Fukue

⋆ sanghamitra@iitb.ac.in
† phs057110@mail2.iitd.ac.in
‡ akr@iucaa.ernet.in
§ tapas@mri.ernet.in

1987; Chakrabarti 1989, 1990; Kafatos & Yang 1994; Yang & Kafatos 1995; Pariev 1996; Lasota & Abramowicz 1997; Lu et al. 1997; Peitz & Appl 1997; Das 2002; Barai et al. 2004; Das 2004; Abraham et al. 2006; Das et al. 2006), as opposed to steady spherically symmetric flows, where, as it is well known, physical transonicity occurs only once (Begelman 1978; Brinkmann 1980; Ray & Bhattacharjee 2002; Mandal et al. 2007). Physical transonic solutions can be represented mathematically as critical solutions in the phase plane of the flow, i.e. they are associated with critical points — alternatively known as fixed points or equilibrium points (Jordan & Smith 1999). These solutions may even pass through critical points (as, for instance, a flow through a saddle point). In this situation much information about various physical properties of accretion processes could be gleaned if these critical points are analysed carefully, which is the central objective of this work.

In this treatment the nonlinear equations describing the steady, inviscid, rotational, axisymmetric flow in the Kerr metric, have been tailored to form a first-order autonomous dynamical system (Jordan & Smith 1999). The critical points of the phase trajectories of the flow have been identified first, following which, a linearised study in the neighbourhood of these critical points has been carried out. As a consequence of this exercise, a complete and rigorous mathematical classification scheme for the nature of the critical points has been derived, and it has been argued that the critical points can admissibly be only saddle points and centre-type points for the kind of conserved, axisymmetric and rotational flow under study here. While all of these are principally the attributes of the hydrodynamical process itself, the influence of the black hole (the agent external to the fluid, but driving its flow nonetheless) has also been noteworthy to the extent that its intrinsic rotational parameter affects the character of multitransonicity in general and the properties of an individual critical point in particular. This is an important result to have emerged from the study.

As a special case of what has been done in the Kerr geometric space-time, a similar study has also been carried out for the flow in the metric of a non-rotating Schwarzschild black hole. The results are entirely in keeping with the usual expectations formed on the basis of the conclusions drawn from the analysis carried out for the Kerr metric.

Global understanding of the flow topologies will necessitate a full numerical integration of the nonlinear equations of the flow. This is never an easy task, but equipped with a clear analytical conception of the local features of the critical points of the flow, it becomes possible to qualitatively anticipate the nature of the global behaviour of solutions. In fact, if the system has no more than two critical points, then with some knowledge of the physical boundary conditions of the flow, absolutely correct qualitative predictions can be made about the solution topologies (Ray & Bhattacharjee 2002, 2007).

Particularly with respect to accretion on to black holes, this work follows two earlier works in studying critical properties of accretion solutions, with the aid of the mathematical tools of a dynamical systems approach. One work was devoted to discussing the behaviour of critical points in a steady, axisymmetric, rotational flow, driven towards the central black hole in the pseudo-Schwarzschild framework (Chaudhury et al. 2006). The second work dealt with transonicity and its associated aspects in a fully general relativistic, spherically symmetric flow described by the Schwarzschild metric (Mandal et al. 2007). The present work on rotational flows in the Kerr metric may be seen as an extension of these earlier efforts, and it gives an example of the relative mathematical ease with which otherwise difficult physical questions in general relativistic fluid dynamical problems may be confronted.

2 THE STATIONARY FLOW IN THE KERR METRIC AND ITS FIXED POINTS

Neglecting the self-gravity of this general relativistic, axisymmetric, inviscid, stationary, compressible hydrodynamic flow in the Kerr geometric space-time, the conserved equation for the specific flow energy, $\mathcal{E}$, can be expressed as (Anderson 1989; Barai et al. 2004; Das et al. 2006)

$$\mathcal{E} = hv_t, \tag{1}$$

which is actually the relativistic analogue of Bernoulli's equation. The specific enthalpy, h, can be defined as

$$h = \frac{p+\epsilon}{\rho}, \tag{2}$$

with ϵ, which contains the rest mass density and the internal energy, being further given by,

$$\epsilon = \rho + \frac{p}{\gamma - 1}. \tag{3}$$

The pressure, p, is expressed as a function of the density, ρ, through an equation of state, $p = k\rho^{\gamma}$, from which, under conditions of constant entropy, $\mathcal{S}$, the speed of sound is defined as

$$c_{\rm s}^2 = \left.\frac{\partial p}{\partial \epsilon}\right|_{\mathcal{S}}. \tag{4}$$

All of these establish a connection between the density, ρ, and the speed of sound, $c_{\rm s}$, as

$$\rho = \left[\frac{c_{\rm s}^2}{\gamma k\left(1 - n c_{\rm s}^2\right)}\right]^n, \tag{5}$$

with n, the polytropic index, being defined as $n = (\gamma - 1)^{-1}$. This will subsequently lead to an expression of the specific enthalpy in terms of $c_{\rm s}^2$ as

$$h = \frac{1}{1 - nc_{\rm s}^2}. \tag{6}$$

A further definition gives v_t as

$$v_t = \sqrt{\frac{f(r)}{1 - v^2}}, \tag{7}$$

in which v is the radial three-velocity of the corotating fluid (Barai et al. 2004; Das et al. 2006). The function $f(r)$ is defined as

$$f(r) = \frac{Ar^2\Delta}{A^2 - 4\lambda arA + \lambda^2 r^2(4a^2 - r^2\Delta)},$$

with $A(r) = r^4 + r^2a^2 + 2ra^2$ and $\Delta(r) = r^2 - 2r + a^2$. In all of these, the fixed parameters λ and a are the sub-Keplerian specific angular momentum of the flow and the rotating Kerr parameter, respectively. Following these definitions, a final expression for the relativistic Bernoulli equation will be derived as

$$\mathcal{E} = \frac{1}{1 - nc_{\rm s}^2}\sqrt{\frac{f(r)}{1 - v^2}}. \tag{8}$$

From the continuity condition, the other governing equation of the flow will be obtained as (Barai et al. 2004; Das et al. 2006)

$$4\pi\Delta^{1/2}H\rho\sqrt{\frac{v^2}{1 - v^2}} = \dot{m}, \tag{9}$$

in which the integration constant, $\dot{m}$, is the physical matter flow rate. The height of the thin disc flow, $H(r)$, under conditions of hydrostatic equilibrium in the vertical direction, is expressed as (Barai et al. 2004; Das et al. 2006)

$$H(r) = \sqrt{\frac{2}{\gamma}}r^2\left[\frac{c_{\rm s}^2}{(1 - nc_{\rm s}^2)\left\{\lambda^2 v_t^2 - a^2\left(v_t - 1\right)\right\}}\right]^{1/2}. \tag{10}$$

Making use of equations (5) and (10) in equation (9), and eliminating the derivatives of $c_{\rm s}$ with the help of equation (8), it becomes possible, under the definition that $g_1(r) = \Delta r^4$ and $g_2(r, v^2) = \lambda^2 v_t^2 - a^2 v_t + a^2$, to arrive at the relation

$$\left[\frac{1}{1 - v^2}\left(1 - \frac{\beta^2 c_{\rm s}^2}{v^2}\right) + \frac{\beta^2 c_{\rm s}^2}{g_2}\left(\frac{\partial g_2}{\partial v^2}\right)\right]\frac{\rm d}{{\rm d}r}(v^2) = \beta^2 c_{\rm s}^2\left[\frac{g_1'}{g_1} - \frac{1}{g_2}\left(\frac{\partial g_2}{\partial r}\right)\right] - \frac{f'}{f}, \tag{11}$$

in which $\beta^2 = 2(\gamma + 1)^{-1}$, and the primes represent full derivatives with respect to r.

From the form of equation (11) it is easy to appreciate that it is a first-order nonlinear autonomous differential equation, whose integration will give the integral solutions in the r — v^2 plane. The critical points of these solutions will be derived by the simultaneous vanishing of the right hand side of equation (11) and the coefficient of ${\rm d}(v^2)/{\rm d}r$ in the left hand side. This will give the two critical point conditions as

$$\beta^2 c_{\rm sc}^2\left[\frac{g_1'(r_{\rm c})}{g_1(r_{\rm c})} - \frac{1}{g_2(r_{\rm c}, v_{\rm c}^2)}\left(\frac{\partial g_2}{\partial r}\right)\bigg|_{\rm c}\right] - \frac{f'(r_{\rm c})}{f(r_{\rm c})} = 0 \tag{12}$$

and

$$\frac{1}{1 - v_{\rm c}^2}\left(1 - \frac{\beta^2 c_{\rm sc}^2}{v_{\rm c}^2}\right) + \frac{\beta^2 c_{\rm sc}^2}{g_2(r_{\rm c}, v_{\rm c}^2)}\left(\frac{\partial g_2}{\partial v^2}\right)\bigg|_{\rm c} = 0, \tag{13}$$

respectively, with the subscript "c" indicating the values at the critical points.

To fix the critical points in terms of the flow parameters, it will be first necessary to make use of both equations (12) and (13) to eliminate $c_{\rm sc}^2$. Following this, some simple algebraic manipulations, with the help of the definition of $g_2(r, v^2)$ will make it possible to express $v_{\rm c}^2$ entirely as a function of $r_{\rm c}$, and this will be given by

$$v_{\rm c}^2 = \frac{f'(r_{\rm c})g_1(r_{\rm c})}{f(r_{\rm c})g_1'(r_{\rm c})}. \tag{14}$$

It will then be possible, with the aid of either equation (12) or equation (13), to express $c_{\rm sc}^2$ as a function of $r_{\rm c}$ only, and all these conditions, substituted in equation (8), will deliver the roots of $r_{\rm c}$ in terms of $\mathcal{E}$, λ, γ and a. The critical points will, therefore, become fixed in the r — v^2 plane.

3 NATURE OF THE FIXED POINTS : AN AUTONOMOUS DYNAMICAL SYSTEM

Quite frequently for any nonlinear physical system, a linearised analytical study of the properties of the fixed points affords a robust platform for carrying out an investigation to understand the global behaviour of integral solutions in the phase portrait. This is especially useful in the absence of any well-prescribed and general means of solving nonlinear differential equations, which, perforce, have to be solved numerically.

It has already been shown that the stationary, axisymmetric, rotational flow in the Kerr metric can be reduced to a first-order autonomous system, and as such it lends itself easily to a dynamical systems study of its fixed points. To do so, it should be necessary to decompose equation (11) into two parametrized equations, given by

$$\begin{aligned}\frac{\mathrm{d}}{\mathrm{d}\tau}(v^2) &= \beta^2 c_{\rm sc}^2\left[\frac{g_1'}{g_1}-\frac{1}{g_2}\left(\frac{\partial g_2}{\partial r}\right)\right]-\frac{f'}{f}\\ \frac{\mathrm{d}r}{\mathrm{d}\tau} &= \frac{1}{1-v^2}\left(1-\frac{\beta^2 c_{\rm sc}^2}{v^2}\right)+\frac{\beta^2 c_{\rm sc}^2}{g_2}\left(\frac{\partial g_2}{\partial v^2}\right),\end{aligned} \tag{15}$$

in which τ is a mathematical parameter. Since equations (15) are autonomous equations, τ does not explicitly appear in their right hand sides (Jordan & Smith 1999).

This kind of parametrization represents the first step towards carrying out a linear stability analysis of the fixed points of a nonlinear system, and for the present treatment on disc flows in the Kerr geometric space-time, this will give a complete classification scheme for the critical points of the flow. In general fluid dynamics problems — all of which are nonlinear problems — this approach is quite common (Bohr et al. 1993), and in the context of accretion studies (which, in its essence, is the study of a compressible fluid flow), this method has been quite effectively adopted before (Ray & Bhattacharjee 2002; Afshordi & Paczyński 2003; Chaudhury et al. 2006; Mandal et al. 2007). Some earlier works in accretion had also made use of the general mathematical aspects of this approach (Matsumoto et al. 1984; Muchotrzeb-Czerny 1986; Abramowicz & Kato 1989).

Making use of the perturbation scheme, $v^2 = v_{\rm c}^2 + \delta v^2$, $c_{\rm s}^2 = c_{\rm sc}^2 + \delta c_{\rm s}^2$ and $r = r_{\rm c} + \delta r$, along with a modified form of the continuity condition,

$$\frac{\delta c_{\rm s}^2}{c_{\rm sc}^2} = \mathcal{A}\,\delta v^2 + \mathcal{B}\,\delta r, \tag{16}$$

in which

$$\mathcal{A} = -\frac{\gamma-1-c_{\rm sc}^2}{\gamma+1}\left[\frac{1}{v_{\rm c}^2\left(1-v_{\rm c}^2\right)}-\frac{1}{g_2(r_{\rm c},v_{\rm c}^2)}\left(\frac{\partial g_2}{\partial v^2}\right)\Bigg|_{\rm c}\right]$$

and

$$\mathcal{B} = -\frac{\gamma-1-c_{\rm sc}^2}{\gamma+1}\left[\frac{g_1'(r_{\rm c})}{g_1(r_{\rm c})}-\frac{1}{g_2(r_{\rm c},v_{\rm c}^2)}\left(\frac{\partial g_2}{\partial r}\right)\Bigg|_{\rm c}\right],$$

it is a straightforward exercise to establish a coupled linear dynamical system in the perturbed quantities δv^2 and δr. This is given by

$$\begin{aligned}\frac{\mathrm{d}}{\mathrm{d}\tau}(\delta v^2) &= \beta^2 c_{\rm sc}^2\left[\frac{\mathcal{A}g_1'}{g_1}-\frac{\mathcal{A}\mathcal{C}}{g_2}+\frac{\mathcal{C}\mathcal{D}}{g_2^2}-\frac{\Delta_3}{g_2}\right]\delta v^2\\ &\quad+\left[\frac{\beta^2 c_{\rm sc}^2 g_1'}{g_1}\left\{\mathcal{B}+\left(\frac{g_1''}{g_1'}-\frac{g_1'}{g_1}\right)\right\}-\frac{f'}{f}\left(\frac{f''}{f'}-\frac{f'}{f}\right)-\frac{\beta^2 c_{\rm sc}^2\mathcal{C}}{g_2}\left(\mathcal{B}-\frac{\mathcal{C}}{g_2}+\frac{\Delta_4}{\mathcal{C}}\right)\right]\delta r\\ \frac{\mathrm{d}r}{\mathrm{d}\tau} &= \left[\frac{1}{\left(1-v_{\rm c}^2\right)^2}-\frac{\beta^2 c_{\rm sc}^2}{v_{\rm c}^2\left(1-v_{\rm c}^2\right)}\left\{\mathcal{A}+\frac{2v_{\rm c}^2-1}{\left(1-v_{\rm c}^2\right)^2}\right\}+\frac{\beta^2 c_{\rm sc}^2\mathcal{D}}{g_2}\left(\mathcal{A}-\frac{\mathcal{D}}{g_2}+\frac{\Delta_1}{\mathcal{D}}\right)\right]\delta v^2\\ &\quad+\left[-\frac{\beta^2 c_{\rm sc}^2\mathcal{B}}{v_{\rm c}^2\left(1-v_{\rm c}^2\right)}+\frac{\beta^2 c_{\rm sc}^2\mathcal{D}}{g_2}\left(\mathcal{B}-\frac{\mathcal{C}}{g_2}+\frac{\Delta_2}{\mathcal{D}}\right)\right]\delta r,\end{aligned} \tag{17}$$

in which f, g_1 and g_2, all of which are contained in the constant coefficients of the perturbed quantities, are to be read at the critical points only. Explicitly written, all the newly appeared constants in the coefficients of equations (17) are to be given as

$$\mathcal{C} = \left(\frac{\partial g_2}{\partial r}\right)\Bigg|_{\rm c}, \qquad \mathcal{D} = \left(\frac{\partial g_2}{\partial v^2}\right)\Bigg|_{\rm c},$$

$$\Delta_1 = \frac{\partial}{\partial v^2}\left(\frac{\partial g_2}{\partial v^2}\right)\Bigg|_{\rm c}, \qquad \Delta_2 = \frac{\partial}{\partial r}\left(\frac{\partial g_2}{\partial v^2}\right)\Bigg|_{\rm c}, \qquad \Delta_3 = \frac{\partial}{\partial v^2}\left(\frac{\partial g_2}{\partial r}\right)\Bigg|_{\rm c}, \qquad \Delta_4 = \frac{\partial}{\partial r}\left(\frac{\partial g_2}{\partial r}\right)\Bigg|_{\rm c}.$$

Using solutions of the kind $\delta v^2 \sim \exp(\Omega\tau)$ and $\delta r \sim \exp(\Omega\tau)$, the eigenvalues of the stability matrix corresponding to equations (17), can be set down as

$$\Omega^2 = \beta^4 c_{\rm sc}^4 \chi^2 + \xi_1 \xi_2, \tag{18}$$

in which

$$\chi = \left[\frac{g_1' \mathcal{A}}{g_1} - \frac{\mathcal{A}\mathcal{C}}{g_2} + \frac{\mathcal{C}\mathcal{D}}{g_2^2} - \frac{\Delta_3}{g_2} \right] = \left[\frac{\mathcal{B}}{v_{\rm c}^2 \left(1 - v_{\rm c}^2\right)} - \frac{\mathcal{B}\mathcal{D}}{g_2} + \frac{\mathcal{C}\mathcal{D}}{g_2^2} - \frac{\Delta_2}{g_2} \right],$$

$$\xi_1 = \frac{\beta^2 c_{\rm sc}^2 g_1'}{g_1} \left[\mathcal{B} + \frac{g_1''}{g_1'} - \frac{g_1'}{g_1} \right] - \frac{f'}{f} \left[\frac{f''}{f'} - \frac{f'}{f} \right] - \frac{\beta^2 c_{\rm sc}^2 \mathcal{C}}{g_2} \left[\mathcal{B} - \frac{\mathcal{C}}{g_2} + \frac{\Delta_4}{\mathcal{C}} \right]$$

and

$$\xi_2 = \frac{1}{\left(1 - v_{\rm c}^2\right)^2} - \frac{\beta^2 c_{\rm sc}^2}{v_{\rm c}^2 \left(1 - v_{\rm c}^2\right)} \left[\mathcal{A} + \frac{2v_{\rm c}^2 - 1}{v_{\rm c}^2 \left(1 - v_{\rm c}^2\right)} \right] + \frac{\beta^2 c_{\rm sc}^2 \mathcal{D}}{g_2} \left[\mathcal{A} - \frac{\mathcal{D}}{g_2} + \frac{\Delta_1}{\mathcal{D}} \right]$$

with f, g_1 and g_2 to be read once again at the critical points.

The form of equation (18) indicates that the critical points can only be either saddle points (when $\Omega^2 > 0$) or centre-type points (when $\Omega^2 < 0$), which is just what they should be for a system that is conservative in nature (Jordan & Smith 1999). The properties of a critical point could be ascertained by making use of the critical point coordinates, $(r_{\rm c}, v_{\rm c}^2)$, in equation (18), to find the corresponding value of Ω^2, and more especially, its sign. This knowledge, along with known and physically meaningful boundary conditions of the flow, will give a clear idea of the local behaviour of the integral solutions in the vicinity of the critical points. If the system is simple enough, i.e. if it has one or at most two critical points, then a complete qualitative impression of the global behaviour of the solutions can be obtained from this simple analytical exercise (Ray & Bhattacharjee 2002, 2007). Occasionally these situations can actually arise in thin disc flows (relativistic or otherwise) for certain values of the relevant flow parameters (Das et al. 2006). And this is almost certainly true for relatively simple spherically symmetric flows (Ray & Bhattacharjee 2002; Mandal et al. 2007).

4 THE SCHWARZSCHILD LIMIT

The study carried out so far has been in the Kerr geometric space-time. Although this is a very general case of a relativistic astrophysical flow, of no less interest — especially from a theoretical viewpoint — is the case of relativistic axisymmetric flows in a spherically symmetric metric. This limit — the Schwarzschild limit — is to be achieved by simply making the Kerr parameter vanish ($a = 0$) in equations (8), (9) and (10). This will make the black hole a non-rotating accretor, and in the space-time described by its gravity, the relativistic Bernoulli equation will be expressed as

$$\mathcal{E} = \frac{1}{1 - nc_{\rm s}^2} \sqrt{\frac{r^2 \left(r - 2\right)}{\left(1 - v^2\right) \left[r^3 - \lambda^2 \left(r - 2\right)\right]}}, \tag{19}$$

while the thickness of the disc, $H(r)$, will go as (Das et al. 2006)

$$H(r) = \sqrt{\frac{2}{\gamma}} \frac{r^2 c_{\rm s}}{\lambda} \left[\frac{\left(1 - v^2\right) \left\{r^3 - \lambda^2 \left(r - 2\right)\right\}}{\left(1 - nc_{\rm s}^2\right) r^2 \left(r - 2\right)} \right]^{1/2}. \tag{20}$$

The equation of continuity will retain the same form as equation (9) even in the Schwarzschild metric, and making use of equations (5) and (20) in equation (9), it should be possible to recast the equation of continuity in a suitable form as

$$\frac{\rm d}{{\rm d}r}(c_{\rm s}^2) = -2c_{\rm s}^2 \left(\frac{\gamma - 1 - c_{\rm s}^2}{\gamma + 1} \right) \left[\frac{1}{2v^2} \frac{\rm d}{{\rm d}r}(v^2) + f_1(r) \right], \tag{21}$$

with f_1 defined as

$$f_1(r) = \frac{3r^3 - 2\lambda^2 r + 3\lambda^2}{r^4 - \lambda^2 r \left(r - 2\right)}.$$

Following this, it will become quite easy to derive an expression for the gradient of solutions in the r — v^2 plane, and this will read as

$$\left[\frac{1}{1 - v^2} - \frac{\beta^2 c_{\rm s}^2}{v^2} \right] \frac{\rm d}{{\rm d}r}(v^2) = 2\beta^2 c_{\rm s}^2 f_1(r) - 2f_2(r) \tag{22}$$

with f_2 being given further by the definition

$$f_2(r) = \frac{2r - 3}{r \left(r - 2\right)} - \frac{2r^3 - \lambda^2 r + \lambda^2}{r^4 - \lambda^2 r \left(r - 2\right)}.$$

The critical points (labelled by the subscript "c") could be read from the critical conditions delivered by equation (22) as

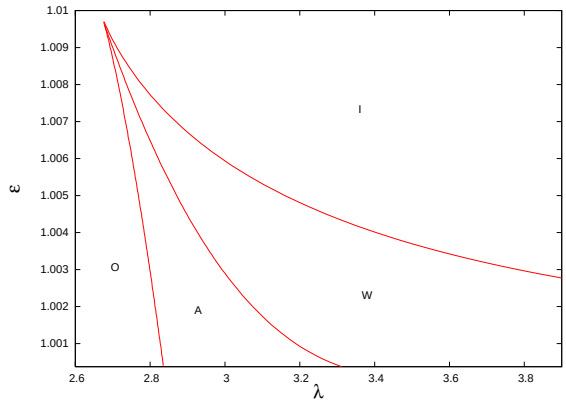

Figure 1. Regions of multitransonicity for both accretion (marked A) and wind (marked W) in the parameter space of $\mathcal{E}$ and λ. The labels I and O indicate the regions of the lone inner and outer critical points, respectively. The plot has been generated for $a = 0.3$ and $\gamma = 1.33$.

$$\frac{v_{\rm c}^2}{1-v_{\rm c}^2} = \beta^2 c_{\rm sc}^2 = \frac{f_2(r_{\rm c})}{f_1(r_{\rm c})}. \tag{23}$$

From the form of the critical points in the foregoing expressions, it is quite evident that with the help of equation (19), the critical point coordinates can be fixed in terms of $\mathcal{E}$, λ and γ. To understand the behaviour of the critical points, equation (22) would have to be parametrized according to the prescription outlined in Section 3. This will entail writing

$$\begin{aligned} \frac{\mathrm{d}}{\mathrm{d}\tau}(v^2) &= 2\beta^2 c_{\rm s}^2 f_1(r) - 2f_2(r) \\ \frac{\mathrm{d}r}{\mathrm{d}\tau} &= \frac{1}{1-v^2} - \frac{\beta^2 c_{\rm s}^2}{v^2}, \end{aligned} \tag{24}$$

following which, imposing small first-order perturbations about the critical point coordinates, the eigenvalues of the stability matrix of the resulting linearised coupled dynamical system, will be derived as

$$\Omega^2 = (f_1+f_2)^2 \left[\left(2\frac{\gamma-1}{\gamma+1} - \frac{f_2}{f_1} \right)^2 + \frac{2}{f_1} \left(\frac{2\gamma}{\gamma+1} + \frac{1}{2}\frac{f_2}{f_1} \right) \left\{ \frac{f_1'}{f_1} - \frac{f_2'}{f_2} - f_1 \left(2\frac{\gamma-1}{\gamma+1} - \frac{f_2}{f_1} \right) \right\} \right], \tag{25}$$

in which the arguments of the functions f_1 and f_2 will be $r_{\rm c}$, with the primes representing full derivatives with respect to r, as usual. With each physically admissible value of $r_{\rm c}$, the nature of the corresponding critical point will be known from equation (25), and just like the flow in the Kerr metric, the critical points will be seen to be only either saddle points or centre-type points. They could not have been very different, since the treatment on flows in the Schwarzschild metric is anyway a special case of the flow in Kerr space-time. Nevertheless, flows in Schwarzschild geometry merit a separate investigation in their own right, and indeed, for spherically symmetric flows, this special case affords a very clear pedagogical model to understand various accretion-related phenomena, with some surprisingly new features revealed (Mandal et al. 2007).

5 PARAMETER DEPENDENCE OF MULTITRANSONICITY : GENERAL FEATURES

In the two foregoing sections, it has been discussed that for the disc flow in the Kerr metric (and for its Schwarzschild limit as well), the eigenvalues of the stability matrix associated with each of the critical points can be fixed in terms of the relevant parameters of the flow $\mathcal{E}$, λ, γ and a. This obviously implies that the critical behaviour of the flow can actually be determined by these parameters. Multitransonicity is one very important critical feature of the flow and its dependence on the parameters $\mathcal{E}$ and λ in this Kerr geometric system (for fixed values of γ and a) has been depicted in Fig. 1.

The region marked by O corresponds to a single outer critical point at large length scales. This occurs for low values of λ and $\mathcal{E}$. It is not difficult to intuitively grasp the reason for this. Gravity drives the accretion process, and this is manifested by the growth of the velocity field. In a rotating flow angular momentum acts against the interest of gravity, and depending on the strength of the presence of angular momentum, the velocity field will develop accordingly. Criticality in the flow is achieved when its velocity matches the speed of acoustic propagation in the fluid. The resistance raised due to the presence of low angular momentum in the rotating fluid can, therefore, be overcome even at large distances (where gravity is comparatively weak). Besides this, a low value of $\mathcal{E}$ will imply that the compressible fluid is "cold" and as such it cannot offer much of a resistance against gravity with the help of its internal thermal effects. And so once again gravity wins easily, with criticality developing at large length scales. All of these features are manifested in the region marked O in Fig. 1.

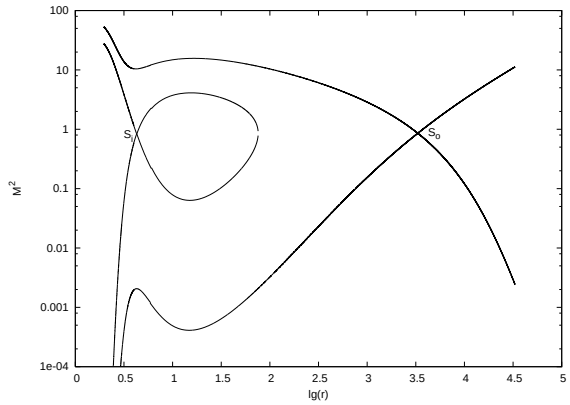

Figure 2. Integral solutions of equation (11), representing region A in Fig. 1. The vertical axis plots M^2 (since it is convenient to measure the bulk velocity against the local speed of sound). Both the axes have been scaled logarithmically for better graphical resolution of the plot. The inner saddle point, S_i, is connected to itself through a homoclinic path. The solutions have been generated for $\mathcal{E} = 1.0001$, $\lambda = 3.15$, $a = 0.3$ and $\gamma = 1.33$.

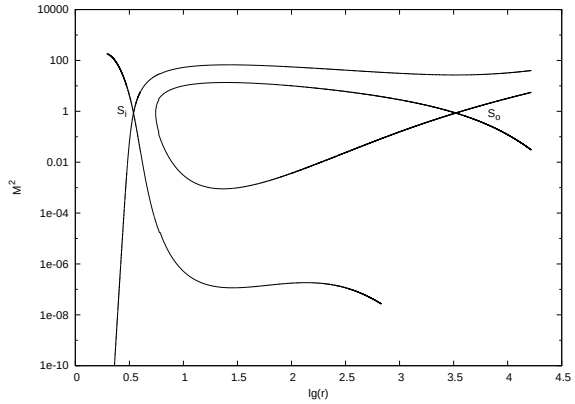

Figure 3. Integral solutions of equation (11), representing region W in Fig. 1. The outer saddle point, S_o, is on a homoclinic path. The solutions have been generated for $\mathcal{E} = 1.0001$, $\lambda = 3.6$, $a = 0.3$ and $\gamma = 1.33$.

On the other hand, when both $\mathcal{E}$ and λ are high, their resistive effects can only be overcome with the rotating fluid having to fall deeper within the potential well, and, therefore, criticality can be attained only at small length scales, in the vicinity of the event horizon of the black hole. This feature has been shown in the region (corresponding to higher values of λ and $\mathcal{E}$) marked I in Fig. 1. All of these arguments can be appreciated much more easily for rotational flows in the non-relativistic and Newtonian representation. One might expect that the qualitative character of the physics in this regime, should also carry over smoothly to the general relativistic case. At least the parameter space representation in Fig. 1 does nothing to make one believe otherwise, because a similar pattern is also exhibited for non-relativistic pseudo-Newtonian flows (Das 2002).

The multitransonic aspect of the flow has been shown by the wedge-shaped region in Fig. 1. This region has been further subdivided into two regions, marked by A (accretion) and W (wind). To gain an understanding of the physical criterion behind this subdivision, it should be necessary first to go to equation (9), and then substitute ρ in it in terms of c_s, with the help of equation (5). This process will lead to the defining of a new parameter for the flow, $\dot{\mathcal{M}} = (\gamma k)^n \dot{m}$. This newly defined parameter is physically understood to be the entropy accretion rate.

Now multitransonicity in this Kerr geometric flow implies the existence of three critical points, and under the fundamental physical requirement of accretion being a process whereby a flow solution should connect infinity to the event horizon of the black hole, the three critical points should be such that there would be two saddle points flanking a centre-type point between themselves. Going back to Fig. 1, the criterion to distinguish region A (the accretion region) will be that the entropy accretion rate, $\dot{\mathcal{M}}_{\rm in}$, through the inner saddle point must be greater than the corresponding flow rate, $\dot{\mathcal{M}}_{\rm out}$, through the outer saddle point. The exact reversal of this argument, i.e. $\dot{\mathcal{M}}_{\rm out} > \dot{\mathcal{M}}_{\rm in}$, will define the region W (the wind region) in Fig. 1.

The former situation can be understood very clearly from Fig. 2, in which the integral solutions of equation (11) have been drawn under various boundary conditions. The vertical axis plots M^2 (with M, the Mach number, being defined as $M = v/c_s$) against the radial distance along the horizontal axis. The behaviour of the solution passing through the inner saddle point, S_i, (whose associated value of $\dot{\mathcal{M}}$ is greater than its corresponding value for the outer saddle point, S_o) is most interesting. It

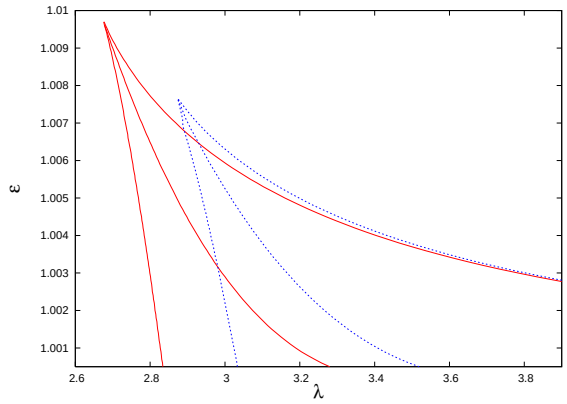

Figure 4. A comparison of the multitransonic regions in the parameter space of $\mathcal{E}$ and λ, for two different values of a, and with $\gamma = 1.33$. The dotted curves (coloured blue in the online version) are for $a = 0$ (the Schwarzschild limit). The continuous curves (coloured red in the online version) are for $a = 0.3$. For the latter case, the shift of the multitransonic region towards lower values of λ and higher values of $\mathcal{E}$ is quite evident. The area of multitransonicity also increases with the increase in the value of a.

connects the point S_i to itself through a loop, and hence, to invoke the terminology of plane autonomous dynamical systems, this solution is actually a homoclinic path (Jordan & Smith 1999).

While Fig. 2 depicts the actual behaviour of the phase trajectories corresponding to the wedge-shaped region marked by A in Fig. 1, the converse behaviour of these trajectories, corresponding to the region W (wind) has been shown in Fig. 3. Here the governing principle is that the entropy accretion rate pertaining to the outer saddle point is greater than the one for the inner saddle point (i.e. $\dot{\mathcal{M}}_{\rm out} > \dot{\mathcal{M}}_{\rm in}$), and it is evident from the plot that in this situation the solution passing through the outer saddle point, S_o, is a homoclinic path. So a general conclusion that can be drawn is that for a physical flow such as the one under study here, multitransonicity will imply the existence of a homoclinic path (which is a flow solution that connects a saddle point to itself). The quantitative physical guideline to identify such a solution is to first identify the saddle point through which the entropy accretion rate, $\dot{\mathcal{M}}$, is greater than what it is for any of the other ones.

For accretion in particular, a long-standing understanding has been that the flow has to take place at the maximum possible rate. One could go back to a pioneering work in this subject, in which Bondi (1952) had conjectured that since there would be nothing to prevent the accretion process, it might as well take place at the greatest possible rate, implying that the flow would be transonic. While this conjecture was made on the basis of the spherically symmetric flow, which has a single critical point (a saddle point), it would still be relevant for multitransonic disc flows. Once, after starting under suitable outer boundary conditions, an inflow solution has passed through the outer saddle point, it will then undergo a transition, so that the entropy accretion rate is increased further by the solution passing through the inner saddle point. This transition will occur through a standing shock, and this process defines an unambiguous path for the infalling matter to reach the event horizon of the black hole. Various studies have dealt with many questions in this regard (Chakrabarti 1989; Das et al. 2006), but these details will be beyond the scope of the present study, which is devoted only to the critical aspects of the flow.

A further interesting issue related to Figs. 2 and 3 is that in broad qualitative terms, one is evidently a reversed image of the other. While the solutions in Fig. 2 are characterised by $\dot{\mathcal{M}}_{\rm in} > \dot{\mathcal{M}}_{\rm out}$ through the saddle points, the defining criterion for solutions in Fig. 3 is $\dot{\mathcal{M}}_{\rm out} > \dot{\mathcal{M}}_{\rm in}$. It will then be reasonable to suggest that the accreting system will go through a state in which $\dot{\mathcal{M}}_{\rm in} = \dot{\mathcal{M}}_{\rm out}$. Since integral solutions are allowed to intersect only at the critical points of a dynamical system (Jordan & Smith 1999), this will mean that for the condition $\dot{\mathcal{M}}_{\rm in} = \dot{\mathcal{M}}_{\rm out}$, the two saddle points in the phase portrait will be connected by two heteroclinic paths only (Jordan & Smith 1999). Drawing the phase solutions in this situation, however, will entail a tuning of the flow parameters (and the boundary conditions) with infinite numerical precision, something that should be quite impossible in practice. In Fig. 1 the curve separating region A from region W depicts the condition for heteroclinicity. As a matter of fact, this curve, as well as the two other curves bounding the multitransonic region in Fig. 1, can all be viewed as the loci of various kinds of bifurcation points (Jordan & Smith 1999).

So far the discussion has dwelt on the critical properties of the flow for a fixed value of the Kerr rotating parameter, a. It should now be instructive to consider how the variation of a affects the critical properties, because, for the case of a rotating black hole, apart from its mass (which defines all length scales in the flow), its spin parameter will also leave its imprint on the physics of the accretion process. In Fig. 4, the way in which the spin parameter influences multitransonicity has been shown. The dotted curves delineate the region of multitransonicity in the λ — $\mathcal{E}$ parameter space for $a = 0$ (i.e. the Schwarzschild limit). The continuous curves indicate the multitransonic region for $a = 0.3$. It is very obvious that the onset of multitransonicity takes place at lower values of λ for prograde flows (implied by $a > 0$). Besides this, the multitransonic region is also stretched to higher values of $\mathcal{E}$. All of these lead to the understanding that the Kerr spin parameter (for prograde flows at least) favourably affects the multitransonic character of the flow.

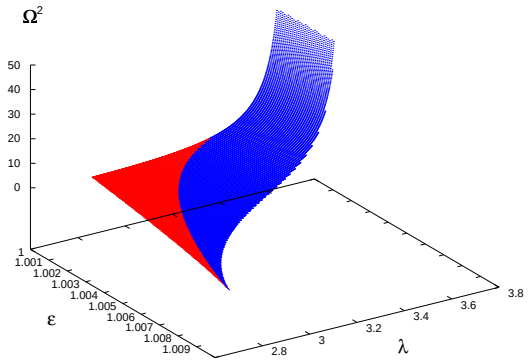

Figure 5. All positive values of Ω^2 indicate that the inner critical point is a saddle point. Its variation in the parameter space of $\mathcal{E}$ and λ has been shown for $a = 0.3$ and $\gamma = 1.33$. The accretion region is given by the lightly shaded area (coloured red in the online version), while the darker region of the surface plot (coloured blue in the online version) indicates wind.

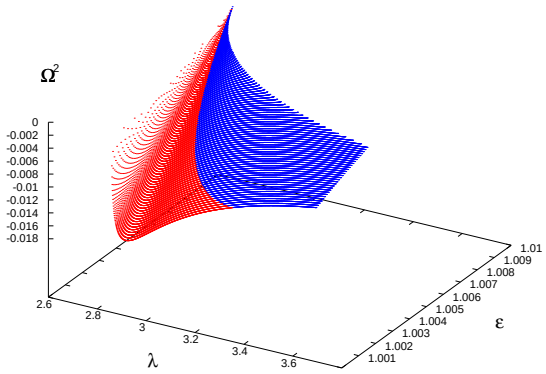

Figure 6. The critical point in the middle is a centre-type point, as the negative values of Ω^2 indicate. The dependence of Ω^2 on $\mathcal{E}$ and λ has been shown for $a = 0.3$ and $\gamma = 1.33$. The colour scheme remains the same as before.

6 PROPERTIES OF THE FIXED POINTS IN MULTITRANSONIC FLOWS

Various general aspects of multitransonicity have been considered in detail by now. To derive some quantitative insight about the specific properties of an individual critical point, however, it will be necessary to go further. The first thing to do in this regard will be to examine the behaviour of the eigenvalues of the stability matrix associated with each critical point. This has to be done by going back to equation (18), which gives a dependence of Ω^2 on the critical point coordinates. These coordinates, in their turn, have a dependence on the parameters $\mathcal{E}$, λ, γ and a. Keeping the last two parameters fixed at

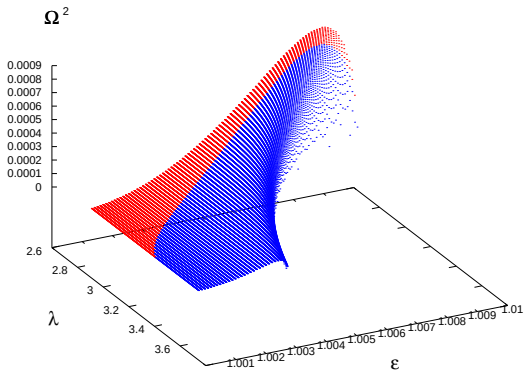

Figure 7. The outer critical point is again a saddle point, since all values of Ω^2 are positive. The dependence of Ω^2 on the parameters $\mathcal{E}$ and λ has been plotted for $a = 0.3$ and $\gamma = 1.33$.

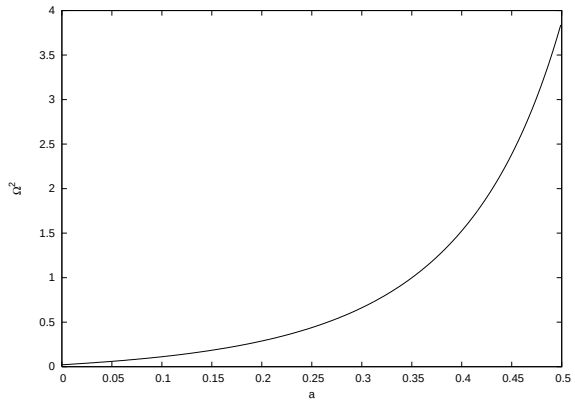

Figure 8. For the inner critical point there is a monotonic growth pattern for the eigenvalues of the stability matrix, Ω^2, with respect to the Kerr parameter, a. The other relevant flow parameters have been fixed at $\mathcal{E} = 1.00035$, $\lambda = 3.05$ and $\gamma = 1.33$. Positive values of Ω^2 indicate that the innermost critical point is always a saddle point. The growth of Ω^2 with increasing a, indicates a strengthening of the saddle-like feature of this critical point.

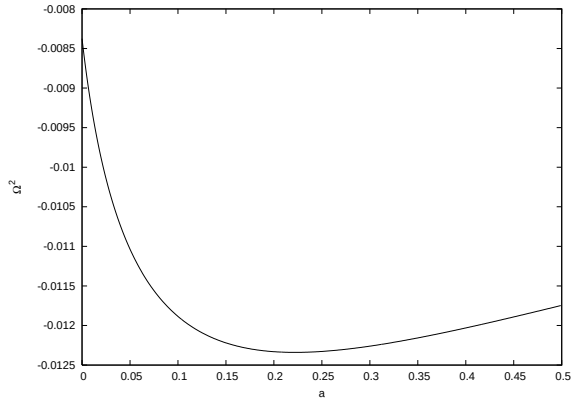

Figure 9. Negative values of Ω^2 indicate that the middle critical point is always a centre-type point. The variation of the eigenvalues shows no monotonic behaviour and there is a minimum near $a = 0.2$. The other flow parameters are $\mathcal{E} = 1.00035$, $\lambda = 3.05$ and $\gamma = 1.33$.

$\gamma = 1.33$ and $a = 0.3$, the variation of Ω^2 with respect to $\mathcal{E}$ and λ, has been plotted in Figs. 5, 6 and 7, for the inner, the middle and the outer critical points, respectively. In all these three surface plots the lightly shaded area (coloured red in the online version) represents accretion, while the dark area (coloured blue in the online version) represents wind. It will not be difficult to appreciate that all the three surfaces in Figs. 5, 6 and 7 will have a two-dimensional projection on the λ — $\mathcal{E}$ plot given in Fig. 1.

The sign of Ω^2 indicates the nature of a critical point. When Ω^2 is positive, it will imply the existence of a saddle point. And so from Figs. 5 and 7, with Ω^2 being positive all the time in these two plots, it is very much evident that the inner and the outer critical points are saddle points for a multitransonic flow. Which is exactly how it should be to make the whole accretion process feasible, because otherwise there will be no open path connecting the event horizon of the black hole and the outer boundary of the flow (which, mathematically speaking, will be at infinity). Having made a note of this qualitative similarity between these two critical points, the quantitative differences will also have to be stressed. The first difference is that the respective values of Ω^2 for either saddle point, differ from those of the other by orders of magnitude. The inner saddle point behaves more robustly in this regard. A further difference is that while Ω^2 decreases slightly with increasing $\mathcal{E}$ (at a fixed value of λ) for the inner saddle point (as Fig. 5 shows), the trend is quite the opposite for the outer saddle point. Here, for a fixed value of λ, there is a growth pattern for Ω^2 with increasing $\mathcal{E}$, as Fig. 7 indicates. This growth is quite noticeable when the value of λ is small. For high values of $\mathcal{E}$, however, there is a sharp dip. As opposed to both the critical points in the extremeties, the critical point in the middle is always a centre-type point, a fact that is indicated by the negative values of Ω^2, given in Fig. 6. Once again, like the outer saddle point, Ω^2 increases with increasing $\mathcal{E}$, at a fixed value of λ.

While Figs. 5, 6 and 7 indicate a dependence of Ω^2 on $\mathcal{E}$ and λ for fixed values of a and γ, it will also be necessary to see how Ω^2 varies with a, having all other parameters fixed. This will reveal how the mathematical properties of the critical points are affected by an intrinsic physical property of the black hole. This has been quantitatively represented in Figs. 8, 9 and 10. The two critical points in the extremeties are, of course, saddle points, but once again, in quantitative terms, they behave in

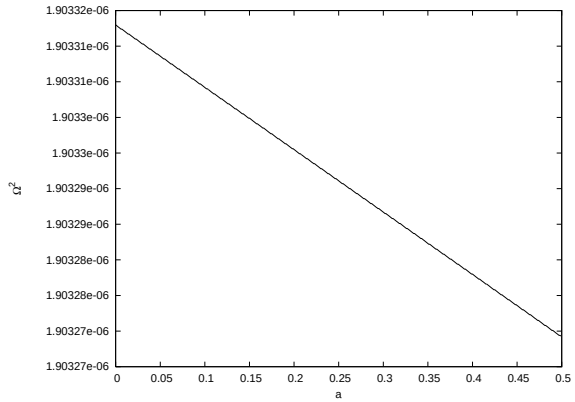

Figure 10. The outer critical point is always a saddle point, as the positive values of Ω^2 indicate. There is a steady decay in the magnitude of Ω^2 with increasing a, which implies a gradual weakening of the saddle-like properties. As usual, the other flow parameters are $\mathcal{E} = 1.00035$, $\lambda = 3.05$ and $\gamma = 1.33$.

a manner contrary to each other. While, for the inner saddle point, Ω^2 grows with increasing values of a (shown in Fig. 8), there is a steady decline in the magnitude of Ω^2 for the outer saddle point (shown in Fig. 10). So, physically speaking, while the presence of the Kerr parameter augments the properties of the inner saddle point, at the same time it has an opposite effect on the outer saddle point. Both these features are, however, manifested in the case of the centre-type point, for which Ω^2 decreases initially with increasing a, reaches a minimum value (near $a = 0.2$), and then starts to increase. These have all been shown in Fig. 9.

7 CONCLUDING REMARKS

While stationary flows are interesting enough, studying the dynamic aspects of the accretion problem reveals new insight related to transonicity, specifically its long-time evolutionary properties and its stability under linearised time-dependent perturbations. These are relatively less complicated ventures to undertake for black hole accretion in the pseudo-Schwarzschild regime, which essentially preserves the simplicity of the Newtonian construct of space and time (Chaudhury et al. 2006). It has been shown for accreting systems, both spherically symmetric and axisymmetric, that generating solutions through a saddle point needs infinitely precise fine-tuning of the boundary condition, but the flow easily attains transonicity if its evolution is traced through time (Ray & Bhattacharjee 2002, 2007). While it may be proposed that this treatment can be extended to proper general relativistic flows, it must also be noted that involving explicit time dependence in a general relativistic fluid flow is always a formidable mathematical problem, more so if the flow is compressible and rotating. If, on the other hand, this could indeed be achieved successfully, then a whole host of interesting new features would emerge. One issue, related particularly to multitransonic flows (which arguably will involve more than one saddle point), is the kind of solution that the temporal evolution will select, that is to say which saddle point will the flow finally choose to reach the event horizon of the black hole, and the physical selection criterion thereof. In this connection other questions like variability and chaotic behaviour (Das et al. 2006) in the flow might also conceivably be brought to the fore.

ACKNOWLEDGEMENTS

This research has made use of NASA's Astrophysics Data System. S. Goswami and S. N. Khan would like to acknowledge the kind hospitality provided by HRI, Allahabad, India, under a visiting students research programme. The authors are also grateful to P. Barai, J. K. Bhattacharjee and S. Nag for much help and some useful comments.

REFERENCES

Abraham, H., Bilić, N., Das, T. K., 2006, Classical and Quantum Gravity, 23, 2371
Abramowicz, M. A., Kato, S., 1989, ApJ, 336, 304
Abramowicz, M. A., Zurek, W. H., 1981, ApJ, 246, 314
Afshordi, N., Paczyński, B., 2003, ApJ, 592, 354
Anderson, M., 1989, MNRAS, 239, 19
Barai, P., Das, T. K., Wiita, P. J., 2004, ApJ, 613, L49

Begelman, M. C., 1978, A&A, 70, 53
Bohr, T., Dimon, P., Putkaradze, V., 1993, J. Fluid Mech., 254, 635
Bondi, H., 1952, MNRAS, 112, 195
Brinkmann, W., 1980, A&A, 85, 146
Chakrabarti, S. K., 1989, ApJ, 347, 365
Chakrabarti, S. K., 1990, Theory of Transonic Astrophysical Flows, World Scientific, Singapore
Chaudhury, S., Ray, A. K., Das, T. K., 2006, MNRAS, 373, 146
Das, T. K., 2002, ApJ, 577, 880
Das, T. K., 2004, MNRAS, 349, 375
Das, T. K., Bilić, N., Dasgupta, S., 2006, arXiv:astro-ph/0604477
Fukue, J., 1987, PASJ, 39, 309
Jordan, D. W., Smith, P., 1999, Nonlinear Ordinary Differential Equations, Oxford University Press, Oxford
Kafatos, M., Yang, R. X., 1994, A&A, 268, 925
Landau, L. D., Lifshitz, E. M., 1987, Fluid Mechanics, Butterworth-Heinemann, Oxford
Lasota, J. P., Abramowicz, M. A., 1997, Classical and Quantum Gravity, 14, A237
Lu, J. F., Yu, K. N., Yuan, F., Young, E. C. M., 1997, A&A, 321, 665
Mandal, I., Ray, A. K., Das, T. K., 2007, arXiv:astro-ph/0702733
Matsumoto, R., Kato, S., Fukue, J., Okazaki, A. T., 1984, PASJ, 36, 71
Muchotrzeb-Czerny, B., 1986, Acta Astronomica, 36, 1
Pariev, V. I., 1996, MNRAS, 283, 1264
Peitz, J., Appl, S., 1997, MNRAS, 286, 681
Ray, A. K., Bhattacharjee, J. K., 2002, Phys. Rev. E, 66, 066303
Ray, A. K., Bhattacharjee, J. K., 2007, Classical and Quantum Gravity, 24, 1
Shapiro, S. L., Teukolsky, S. A., 1983, Black Holes, White Dwarfs, and Neutron Stars, John Wiley & Sons, New York
Yang, R. X., Kafatos, M., 1995, A&A, 295, 238